Published in final edited form as:
Development. 2007 February ; 134(4): 789–799. doi:10.1242/dev.000380.

Convergent extension, planar cell polarity signalling and initiation of mouse neural tube closure

Patricia Ybot-Gonzalez[1], **Dawn Savery**[1], **Dianne Gerrelli**[1], **Massimo Signore**, **Claire E. Mitchell**[2], **Clare H. Faux**[3], **Nicholas D. E. Greene**, and **Andrew J. Copp**[4]
Neural Development Unit, Institute of Child Health, University College London, 30 Guilford Street, London WC1N 1EH, UK

SUMMARY

Planar cell polarity (PCP) signalling is necessary for initiation of neural tube closure in higher vertebrates. In mice with PCP gene mutations, a broad embryonic midline prevents the onset of neurulation through wide spacing of the neural folds. In order to evaluate the role of convergent extension in this defect, we vitally labelled the midline of *loop-tail* (*Lp*) embryos mutant for the PCP gene, *Vangl2*. Injection of DiI into the node, and electroporation of a GFP expression vector into the midline neural plate, reveal defective convergent extension in both axial mesoderm and neuroepithelium, prior to the onset of neurulation. Chimeras containing both wild type and *Lp* mutant cells exhibit mainly wild type cells in the midline neural plate and notochordal plate, consistent with a cell autonomous disturbance of convergent extension. Inhibitor studies in whole embryo culture demonstrate a requirement for signalling via RhoA/Rho kinase, but not jun N-terminal kinase, in convergent extension and the onset of neural tube closure. These findings identify a cell autonomous defect of convergent extension, requiring PCP signalling via RhoA/Rho kinase, during development of severe mouse neural tube defects.

INTRODUCTION

Shaping of the vertebrate embryo during the late stages of gastrulation converts the elliptical gastrula into the keyhole-shaped neurula. This shaping results largely from the cell movements of convergent extension that involve lateral to medial displacement of cells in the plane of the ectoderm, and in the underlying mesoderm (Keller, 2002). Cell intercalation in the midline leads to rostro-caudal extension of the body axis. An essential role in convergent extension has been assigned to the planar cell polarity (PCP) pathway, a highly conserved, non-canonical Wnt/frizzled/dishevelled signalling cascade. PCP signalling plays a key role in establishing and maintaining polarity in the plane of epithelia in *Drosophila*, and in epithelial and non-epithelial tissues in vertebrates (Strutt, 2003; Klein and Mlodzik, 2005).

Both fish and amphibian embryos require an intact PCP pathway for post-gastrulation shaping (Wallingford and Harland, 2001; Park and Moon, 2002; Darken et al., 2002; Jessen et al., 2002). Moreover, in *Xenopus*, PCP-dependent convergent extension in the midline is required for neural tube formation following gastrulation (Wallingford and Harland, 2002; Takeuchi et al., 2003). In its absence, the neural folds are spaced widely apart, precluding the apposition and fusion that is required for neural tube closure (Wallingford and Harland,

[4] Corresponding author: a.copp@ich.ucl.ac.uk; Tel: +44 (0)20 7905 2189.
[1]These authors contributed equally to the work
[2]Current address: Clinical Sciences Centre, Hammersmith Campus, Imperial College London, UK
[3]Current address: Department of Anatomy & Developmental Biology, University College London, UK

Europe PMC Funders Author Manuscripts

2002). A similar failure of initiation of neurulation occurs in several mouse mutants: *loop-tail* (*Lp*), *circletail* (*Crc*), *Crash* (*Crsh*), *protein tyrosine kinase 7* (*Ptk7*), *dishevelled* (*Dvl*) *−1* and *−2* double mutants, and *frizzled* (*Frz*) *−3* and *−6* double mutants (Greene et al., 1998; Murdoch et al., 2001b; Hamblet et al., 2002; Lu et al., 2004; Wang et al., 2006b). This yields the severe defect craniorachischisis (CRN), in which the neural tube remains open from midbrain to low spine (Botto et al., 1999; Copp et al., 1994). CRN comprises up to 10% of human neural tube defects (Moore et al., 1997), and seems likely to result from failure of the initial event of neural tube closure, as in the mouse (Kirillova et al., 2000).

All six of the gene loci associated with CRN in the mouse adversely affect PCP function. The *Lp* mouse is mutant for *Vangl2* (Kibar et al., 2001; Murdoch et al., 2001a), the homologue of *Drosophila strabismus/van gogh*, which encodes a protein that binds directly to dishevelled, participating in its recruitment to the cell membrane (Bastock et al., 2003; Torban et al., 2004). *Crash* mice are mutant for *Celsr1* (Curtin et al., 2003), the homologue of *Drosophila flamingo/starry night*, which plays a role in assembling the PCP protein complex, at least in *Drosophila* (Strutt, 2003). Loss of function of two of the three *dishevelled* genes (*Dsh−1* and *−2*), and two of the six *frizzled* genes (*Frz−3* and *−6*) also leads to CRN (Hamblet et al, 2002; Wang et al, 2006b). Moreover, mutation of *Scrb1* (in *circletail* mice) (Murdoch et al., 2003) and a gene-trap mutation of the tyrosine kinase *Ptk7* (Lu et al, 2004) generate a CRN phenotype. Although not directly implicated in the PCP molecular pathway, both *Scrb1* and *Ptk7* interact genetically with the other mouse CRN genes (Murdoch et al, 2001b; Lu et al, 2004) and produce a planar polarity phenotype in the inner ear (Montcouquiol et al., 2003; Lu et al, 2004). It is striking, therefore, that of the more than 100 genes necessary for neural tube closure in the mouse, all of those with a CRN phenotype disrupt PCP signalling (Copp et al., 2003).

A defect of convergent extension seems likely to precede the failure of neural tube closure in mouse PCP mutants, in view of the widely spaced neural folds described in *Lp*, *Crc*, *Dvl1/2* and *Ptk7* homozygotes (Greene et al, 1998; Murdoch et al, 2003; Lu et al, 2004; Wang et al., 2006a), and the finding of an abnormally short and wide body axis in *Lp/Lp* and *Dvl1/2* embryos during late gastrulation (Wang et al, 2006a). To date, however, a direct analysis of convergent extension in mouse PCP mutants has not been reported. In the present study, we vitally labelled pre-neurulation stage embryos in order to study convergent extension and found that midline extension is defective in both the axial mesoderm and the neural plate of *Lp/Lp* mutants. Analysis of *+/+* ⇔ *Lp/Lp* chimeras suggests a cell autonomous defect in the convergence of *Lp/Lp* cells towards the neural plate midline along the entire body axis, as well as in cells recently emerged from the node, the source of axial mesoderm and midline neural plate in the mouse (Sausedo and Schoenwolf, 1994; Sulik et al., 1994). Among possible signalling pathways downstream of the PCP genes, we find function of RhoA/Rho kinase (ROCK), but not jun N-terminal kinase (JNK), is necessary for convergent extension and initiation of mouse neurulation.

MATERIALS AND METHODS

Mouse strains and genotyping

CD1 random bred mice (Charles River, UK) and CBA/Ca inbred mice (Harlan Olac, UK) provided non-mutant embryos. Heterozygous males of the LPT/Le inbred strain, which carries the *loop-tail* (*Lp*) mutation (Jackson Labs, Bar Harbor, Maine) were mated with CBA/Ca females, and F1 *Lp/+* offspring were intercrossed to generate embryos. *Lp* genotyping was as described (Stanier et al., 1995). The *Crash* (*Crsh*) mutation was originally detected in the F1 generation of ENU-treated strain 101/H males mated with C3H females. *Crsh* genotyping was by PCR amplification of flanking microsatellites D15Mit159 and D15Mit29 (Curtin et al, 2003). The *Circletail* (*Crc*) mutant arose as described (Rachel et al.,

2000), with genotyping by PCR amplification of flanking microsatellites D15Mit144 and D15Mit68 (Murdoch et al, 2001b). Mice homozygous for the gene trap insertions *cordon bleu* (*Cobl*) and ROSA26 were as described (Gasca et al., 1995; Zambrowicz et al., 1997).

Embryo dissection and processing

Embryos were obtained from timed matings; noon on the day of finding a copulation plug was designated 0.5 days of embryonic development (E0.5). Pregnant females were killed by cervical dislocation and embryos were dissected from the uterus in Dulbecco's Modified Eagle's Medium (Gibco, UK) containing 10% fetal calf serum. Embryos for *in situ* hybridisation or histological analysis were washed in phosphate buffered saline (PBS) and fixed in 4% paraformaldehyde (PFA) in PBS at 4°C overnight, or in Bouin's fluid at room temperature for several days. Paraffin wax embedding was followed by sectioning at 8 μm and staining with haematoxylin and eosin. Embryos homozygous for the *cordon bleu* gene trap insertion were stained for bacterial β-galactosidase activity as described (Carroll et al., 2003).

DiI injection into the node of mouse embryos *in vitro*

DiI (1, 1′-dioctadecyl-3, 3, 3′, 3′-tetramethylindocarbocyaninine perchlorate; Molecular Probes, USA) was dissolved in 100% ethanol (0.5 mg/ml), then diluted 10 fold in 3 M sucrose. Node and midline injections were performed at E7.5 (allantoic bud stage) using a hand-held glass micropipette, while viewing the embryo from its posterior (node injection) or anterior (injections rostral to the node) surface, on the stage of a Zeiss SV6 stereomicroscope. The pipette tip was inserted into the node or midline region (Ybot-Gonzalez et al., 2002) and the DiI solution was released as the pipette was slowly withdrawn. Embryos were placed immediately into whole embryo culture.

Electroporation of intact mouse embryos

GFP-expressing constructs were pCAβ-*mGFP6* and pCAβ-IRES-*GFP* (gifts of Dr Jonathan Gilthorpe), in which GFP expression is driven by the chick β-actin promoter under influence of the cytomegalovirus enhancer (Yaneza et al., 2002). Both constructs gave identical GFP-labelling results in embryo electroporation experiments. To prepare a vector expressing constitutively active RhoA, cDNA was amplified from vector pGEX-2T-*RhoA*-Q63L (Self and Hall, 1995) using primers: 5′ GCATATCGATATGGCTGCCATCAGGAAG 3′ and 5′ CAATGCGGCCGCTCACAAGATGAGGCAC 3′. The amplified product was cloned into pGEM-T (Promega, UK) and thence into pCAβ-*mGFP6* to generate vector pCAβ-*RhoA*-IRES-*GFP*, which was verified by DNA sequencing. Constitutively active ROCK, pCAG-myc-P160 ROCK Δ3, wild type ROCK, pCAG-myc-P160 ROCK, and an empty control vector, pCAG-myc, were as described previously (Gutjahr et al., 2005)(gifts of Dr Shuh Narumiya), and were co-electroporated with pCAβ-IRES-*GFP* to enable identification of transfected cells. DNA solution for electroporation contained 4.5 mg/ml pCAβ-*mGFP6* or 2.5 mg/ml other vectors, plus 0.1% Fast Green. E7.5 embryos were placed in phosphate buffered saline (PBS) in a petri dish on a stereomicroscope stage and DNA solution was injected into the amniotic cavity using a hand-held glass micropipette. Embryos were immediately placed between a pair of gold 5 mm point electrodes (BTX model 508) attached to a BTX ECM830 electroporator, with the ventral midline of the caudal embryonic region next to the anode. Current (5 pulses, 50 msec, 15 V) was passed, after which embryos were placed into culture.

Chimera production and analysis

ES cells (129/SvEv; CCE cell line, a gift of Dr Elizabeth Robertson) were injected into E3.5 blastocysts produced from matings between *Lp/+* mice that were also homozygous for the

ROSA26 LacZ marker. Injected blastocysts were transferred to the uterus of E2.5 pseudopregnant recipients, with litters harvested at E8 to obtain chimeras during late gastrulation. After fixation in 4% paraformaldehyde, chimeras were immediately stained as whole mounts by the X-Gal method (Carroll et al, 2003). Transverse sections were prepared following paraffin wax embedding, and cells of each genotype (LacZ-positive or LacZ-negative) were counted in defined areas of midline or lateral neural plate, with focussing at high magnification to distinguish the individual cells. Embryos were genotyped using DNA extracted from yolk sac endoderm, which is entirely host blastocyst-derived (Beddington and Robertson, 1989). Yolk sacs were incubated on ice for 1-5 h in 2.5% pancreatin, 0.5% trypsin in Ca^{2+}/Mg^{2+}-free PBS, after which the endodermal and mesodermal layers were peeled apart.

Inhibitor treatment and analysis of embryos after culture

Embryos were cultured (Copp et al., 1999) with addition of varying concentrations of Y27632 (688000; Calbiochem, UK) dissolved in sterile distilled water (0.5 to 2 μl of 5 mM stock added per ml of rat serum) or SP600125 (420119; Calbiochem, UK) dissolved in dimethyl sulfoxide (0.5 to 2.5 μl of 20 mM stock added per ml of rat serum). At the end of culture, extraembryonic membranes were removed and somites were counted (Copp et al, 1999). Embryos were inspected to determine whether neural tube closure had occurred at the site of Closure 1 (Copp et al, 1994). DiI-injected or electroporated embryos were flat-mounted, dorsal side upwards in PBS on a glass microscope slide and photographed with a Leica DC 500 digital camera on a Leica MZ FLIII stereo-microscope.

In situ hybridisation analysis

Whole mount *in situ* hybridisation, followed by preparation of 50 μm vibratome sections, was performed using digoxygenin-labeled cRNA probes (Copp et al, 1999; Ybot-Gonzalez et al., 2005). Previously published probes were: *JNK1* (Kuan et al., 1999), *Shh* (Greene et al, 1998) and *Vangl2* (Doudney et al., 2005). New cDNA probes were prepared by RT-PCR on total RNA from E10.5 CBA/Ca embryos using TRIzol reagent (Gibco BRL). Amplified fragments were cloned into the pGEM-T vector (Promega, UK) and sequenced to confirm identity. Primer sequences were: *Daam1*: forward 5′ TGCACTTCAGACAATGGAGC 3′ and reverse 5′ ACTCAGAGGTCTCATAGTCC 3′, amplifying a 416 bp fragment (nucleotides 330 to 745; GenBank NM_172464); *RhoA*: forward 5′ CTTTATAAGTGATGGCTGCC 3′ and reverse 5′ TGGTCTTTGCTGAACACTCC 3′, amplifying a 501 bp fragment (nucleotides 11 to 511; GenBank AF178960); *ROCK2*: forward 5′ AGAACACCTTAGCAGTGAGG 3′ and reverse 5′ TTTGGAACTTTCTGCCTGGG 3′, amplifying a 412 bp fragment (nucleotides 1359 to 1770; GenBank U58513).

RT-PCR analysis

RNA was extracted from E7.5, E8.5 and E9.5 CD1 embryos using the PURESCRIPT RNA isolation kit (Gentra Systems, UK), DNA was removed with a DNA-free kit (Ambion, UK), and cDNA was synthesised using a Superscript First Strand Synthesis System (Invitrogen, UK). PCR products were analysed on ethidium bromide-stained 1% agarose gels using Hyperladder I (Bioline, UK) as size markers. Primers were: *LIMK1*: forward 5′ TACCTTTGGAGACGATACCC 3′ and reverse 5′ CCTGATGTACCTGGATTTCC 3′, amplifying a 447 bp fragment (nucleotides 2295 to 2741; GenBank NM_010717); *LIMK2*: forward 5′ CTGTGGATTGAGATTCTGGG 3′ and reverse 5′ TTAGACCCAAAGTCTGAGCC 3′, amplifying a 510 bp fragment (nucleotides 2330 to 2839; GenBank AB008117); *ROCK1*: forward 5′ CAAGCTTGAAGAGCAACTGC 3′ and reverse 5′ CTTGTCTGCTTGTGACTTGG 3′, amplifying a 505 bp fragment (nucleotides 1299 to 1803; GenBank U58512).

Cell culture and immunoblotting

293T cells were cultured by standard methods, plasmids were introduced by calcium phosphate transfection, and cells were lysed in 50 mM Tris pH 7.5, 150 mM NaCl, 1% Triton X100 containing protease inhibitors (Complete; Roche). Protein assays were performed on cell extracts and samples containing 10 μg total protein were electrophoresed. Immunoblots were performed as described previously (Greene et al., 2002), using an antibody for phosphocofilin (1 in 1,000 dilution; Cell Signalling Technology). Blots were stripped and re-probed with an antibody to β-tubulin (1 in 3,000 dilution; Santa Cruz Biotechnology Inc.).

Statistical analysis

Length and width data were subjected to 2-way analysis of variance, with *Lp* genotype and somite number, or presence/absence of ROCK inhibitor and somite number as variables. Response to ROCK and JNK inhibitors (proportion of embryos with open neural tube) was compared between genotypes by z-test. Response to GFP and RhoA/GFP electroporation (proportion of embryos with midline extension) was analysed by chi-square test. All statistics were computed using SigmaStat v.2 (SPSS Inc.).

RESULTS

Defective convergent extension in*Lp* (*Vangl2*) mutant mouse embryos

To determine whether axial extension is compromised in the *loop-tail* (*Vangl2*) mouse mutant, prior to failure of initiation of neural tube closure (Closure 1), we labelled the extending midline by focal injections of DiI into the node at embryonic day (E) 7.5. Embryos of all genotypes were labelled with equal intensity, which was performed blind to embryo genotype (Supplementary Fig. 1A). Following 18 h development in whole embryo culture, rostrally-directed extension of DiI-labelled cells was observed in 94% of wild type embryos (Fig. 1A; Table 1). In contrast, only 47% of *Lp/Lp* embryos exhibited rostral extension, with labelled cells persisting at the site of node injection in the remaining 53% of homozygotes (Fig. 1C). Among *Lp* heterozygotes, 79% showed some rostral extension, but with considerable variability between embryos (Fig. 1B). Embryo sections demonstrate that node injection labels predominantly midline axial mesoderm in the caudal region (Fig. 1G), the notochord along the more rostral body axis (Fig. 1H, I), and midline caudal neural plate in some embryos (Fig. 1G).

As an alternative approach, we labelled midline neural plate cells in the caudal region of E7.5 embryos by electroporation from the amniotic cavity of a DNA vector expressing green fluorescent protein (GFP) under control of the β-actin promoter. GFP expression could be detected from 4 h post-electroporation (Supplementary Fig. 1B). Following 18 h development in whole embryo culture, we observed marked midline extension of GFP-expressing cells in all wild type (Fig. 1D) and in most *Lp/+* embryos (Fig. 1E), whereas all *Lp/Lp* embryos exhibited greatly reduced midline extension (Fig. 1F; Table 1). Staining embryo sections with an anti-GFP antibody confirmed that labelling was in the neural plate (Fig. 1J). These findings demonstrate a defect of convergent extension, affecting both axial mesoderm and neural plate, in pre-neurulation stage homozygous *loop-tail* mutant embryos.

Length and width measurements of DiI-labelled embryos following the culture period also support a defect in convergent extension (Fig. 2A-C). Embryonic length was significantly greater in somite-matched *+/+* embryos compared with *Lp/Lp* littermates, whereas embryonic width showed the reverse trend: *Lp/Lp* embryos were significantly wider than *+/+* littermates. *Lp/+* embryos gave an intermediate result in both cases.

Cell autonomous defect of convergent extension

In *Drosophila*, epithelial PCP effects can be cell autonomous, as in the distal positioning of wing hairs, or non-cell autonomous, as in their long-range polarisation (Strutt, 2003). To investigate the cell autonomy of defective convergent extension in the *Lp* mutant, we constructed chimeras by injecting wild type embryonic stem (ES) cells into blastocysts from *Lp/+* × *Lp/+* matings. Host blastocysts were also homozygous for the ROSA26 LacZ marker, enabling cells of the two genotypes within the chimera to be distinguished in tissue sections. Cells originating from the host blastocyst (LacZ-positive) and from the donor ES cells (LacZ-negative) exhibited an apparently random, fine-grained admixture in both the midline and lateral neural plate of E8 chimeras with *+/+* ⇔ *+/+* genotype (Fig. 3A-C). In contrast, the midline neural plate of *+/+* ⇔ *Lp/Lp* chimeras appeared to contain a lower proportion of LacZ-positive (*Lp/Lp*) cells than lateral regions (Fig. 3D-F). Similarly, we observed a predominance of LacZ-negative cells in the node-derived notochordal plate of *+/+* ⇔ *Lp/Lp* chimeras (Fig. 3D) whereas an even mixture of LacZ-positive and -negative cells was apparent in the notochordal plate of *+/+* ⇔ *+/+* chimeras (Fig. 3A).

To investigate in more detail this apparent genotype-specific difference in colonisation of the midline, we counted the number of LacZ-positive and -negative cells in standardised areas of midline and lateral neural plate at three axial levels in chimeras of *+/+* ⇔ *+/+*, *+/+* ⇔ *Lp/+* and *+/+* ⇔ *Lp/Lp* genotypes (n = 3 embryos per genotype). Individual chimeras are expected to differ from each other in their overall proportion of ES cell-derived and blastocyst-derived components. To eliminate this variation, we subtracted the % LacZ-negative cells in the lateral region from that in the midline of each chimera. Hence, a chimera with similar proportions of the two genotypes in both midline and lateral regions would score zero, and we found that *+/+* ⇔ *+/+* chimeras did indeed yield values clustered around zero (Fig. 3G). In contrast, *+/+* ⇔ *Lp/Lp* chimera sections showed a 15-45% predominance of wild type cells over *Lp/Lp* cells in the midline compared with the lateral neural plate. This effect was present similarly in caudal, middle and cranial regions of the chimeras. Interestingly, a wide variation of values was detected in *+/+* ⇔ *Lp/+* chimeras. Some sections showed a midline-lateral difference close to zero, whereas others showed values similar to those found in *+/+* ⇔ *Lp/Lp* chimeras. We conclude that the colonisation of the midline by *Lp/Lp* cells is intrinsically defective and is not rescued by close juxtaposition to wild type cells in a chimeric combination.

Mechanism underlying defective midline extension in *Lp*

Injection of DiI into the wild type mouse node at E7.5 labels midline chordamesodermal cells along the whole body axis (Fig. 1A)(Beddington, 1994; Sulik et al, 1994). This is consistent with a model derived from avian studies in which Hensen's node ‘regresses’ during gastrulation, laying down the entire notochord (Catala et al., 1996). In mice, a notochord is lacking from embryos following surgical or genetic ablation of the node (Davidson et al., 1999; Ang and Rossant, 1994; Weinstein et al., 1994; Ybot-Gonzalez et al, 2002). Hence, we considered the possibility that the defect of axial extension in *Lp/Lp* embryos may result from a defect in the node. To examine node morphology and gene expression, we bred the *cordon bleu* (*Cobl*) gene trap, which expresses LacZ specifically in the node and its derivatives (Carroll et al, 2003), onto the *Lp* strain. At E7.5, *Lp/Lp* embryos exhibit a LacZ-positive node that is morphologically identical to the wild type node, with closely similar cell numbers (Fig. 4A-D). In contrast, at E8.5, we found a markedly broader LacZ-positive node in *Lp/Lp* embryos than in wild type (Fig. 4E,F). The expression domain of sonic hedgehog (*Shh*) was also broader in the notochord, and particularly in the node and notochordal plate, of *Lp/Lp* embryos compared with *+/+* littermates (Fig. 4G-I). We previously also found a broader expression domain of *brachyury*, in the *Lp/Lp* primitive

streak and node (Greene et al, 1998). These findings suggest a defect of midline cell intercalation in *Lp*, particularly affecting the node and cells recently emerged from the node.

To determine whether notochordal extension at more rostral levels is also affected in *Lp* embryos, we injected DiI at midline positions rostral to the E7.5 node (Fig. 4J-L). Rostral injections label a stream of midline notochordal cells extending variable distances along the body axis, often into the cranial region, but not including the node itself (Fig. 4M-O). In *Lp/Lp* embryos, we observed a similar range of labelling patterns as in wild type and *Lp/+* embryos (Fig. 4P), demonstrating that notochordal extension rostral to the node and notochordal plate are not markedly abnormal in the *Lp* mutant.

Requirement for RhoA/ROCK signalling

We asked whether mouse convergent extension and initiation of neural tube closure require specific signalling downstream of the PCP genes. Signalling via RhoA/ROCK has been identified in *Drosophila*, *Xenopus* and zebrafish (Strutt et al., 1997; Habas et al., 2001; Marlow et al., 2002), and via jun-N-terminal kinase (JNK) in *Drosophila* and *Xenopus* (Boutros et al., 1998; Yamanaka et al., 2002). Moreover, blockade of ROCK function causes defective neural tube closure in the chick (Wei et al., 2001). Reverse transcriptase-PCR shows expression of *RhoA*, *ROCK1* and *ROCK2* from E7.5 to E9.5 of mouse development, together with targets of ROCK phosphorylation including *LIM kinase* (*LIMK*) *−1* and *−2* (Maekawa et al., 1999) (Fig. 5A). *In situ* hybridisation at late gastrulation (E8), when convergent extension is underway, reveals expression of the PCP pathway components *Vangl2*, *Daam1*, *RhoA* and *ROCK2* throughout the embryo (Fig. 5B-E), whereas at E8.5, expression of *Vangl2* and *Daam1* becomes restricted to the region of hindbrain and upper spine, where neural tube closure is initiated (Fig. 5F,G). At this stage, *RhoA*, *ROCK2* and *JNK1* are expressed in domains that overlap with the PCP genes (compare Fig. 5H-J with 5F,G). Transcripts are present in both neural tube and axial/paraxial mesoderm (not shown).

To examine the functional requirement for RhoA/ROCK and JNK signalling in mouse convergent extension and closure initiation, we cultured E7.5 *+/+* and *Lp/+* embryos for 18 h in varying concentrations of the ROCK inhibitor Y27632. Inhibition of ROCK strongly summates with genotype at the *Lp* locus, with *Lp* heterozygotes exhibiting almost 100% open neural tubes even at the lowest concentration of Y27632 tested (2.5 μM). In contrast, 2.5-5 μM inhibitor has no adverse effect on neural tube closure in *+/+* embryos, with non-closure first observed in 50% of embryos only at the near-toxic dose of 10 μM (Fig. 6A; Table 2). We also identified a hallmark of *Lp* homozygotes, a broadened Shh-positive floor plate (Greene et al, 1998), in both *+/+* and *Lp/+* embryos with failed neural tube closure following Y27632 treatment (Fig. 7). Hence, the developmental defect associated with ROCK-dependent failure of Closure 1 resembles that seen in *Lp/Lp*, and seems unlikely to be a non-specific toxic effect.

In contrast to the findings with Y27632, inhibition of JNK activity by SP600125 does not summate with the *Lp* mutation. Both *+/+* and *Lp/+* embryos complete Closure 1 in the presence of inhibitor (Fig. 6B), even at a near-toxic concentration (50 μM) far in excess of that typically used in cell cultures. This result is consistent with the successful Closure 1 seen in mouse embryos lacking function of both *JNK-1* and *−2* (Kuan et al, 1999).

The PCP mutants *Crash* and *Crc* also show an interaction with ROCK inhibition. *Crsh/+* embryos have almost 100% open neural tubes at 2.5 μM Y27632, a concentration that has no effect on *+/+* littermates (Fig. 6C). *Crc/+* embryos are more resistant: open neural tubes first occur at 5 μM Y27632 and, even at 10 μM, only 67% of heterozygotes fail to complete Closure 1 (Fig. 6D). This relative resistance of *Crc/+* embryos to Y27632 may be an effect of genetic background, since wild type littermates are also resistant to Y27632.

Alternatively, the molecular pathway downstream of *Scrb1* may differ subtly from that of the proven PCP genes *Vangl2* and *Celsr1*.

Length and width measurements in *Lp* embryos treated with Y27632 (Fig. 2D,E) reveal a persistent effect of *Lp* genotype similar to embryos cultured without inhibitor. While Y27632 does not affect embryonic length after culture, embryonic width is significantly greater in all genotypes, suggesting that inhibition of RhoA/ROCK signalling may particularly diminish lateral to medial cell movements during gastrulation.

Transfection of active RhoA and ROCK into *Lp* embryos

We attempted to rescue *loop-tail* mutants from CRN by electroporating the midline neural plate with DNA constructs expressing constitutively active forms of RhoA or ROCK. Unexpectedly, both treatments exacerbate the mutant effect, rather than ameliorating it, so that the majority of electroporated *Lp/+* embryos, and even a proportion of *+/+* embryos, fail in Closure 1 like *Lp/Lp* littermates (Table 3). Transfected GFP-positive embryonic cells are sparse and clumped (Fig. 8B,C,E,F) compared with cells electroporated with wild type ROCK (Fig. 8D), or an empty control vector (Fig. 8A), raising the possibility that some cells transfected with active RhoA or ROCK may have died. *In vitro*, 293T cells transfected with active RhoA survive but are rounded, with reduced cellular protrusions (Fig. 8G,H), while immuno-blotting extracts of 293T cells transfected with active RhoA shows diminished abundance of phosphocofilin, a downstream phosphorylation target of the RhoA/ROCK pathway (Fig. 8I). Hence, transfection of constitutively active RhoA or ROCK appears to inhibit downstream signalling, consistent with recent findings (Gutjahr et al, 2005), and providing a likely explanation for the detrimental effect of transfection on neural tube closure.

DISCUSSION

During gastrulation in mammals, two convergent extension processes drive the narrowing and lengthening of the body axis which typifies embryos in the immediate pre-neurulation period. As summarised in Fig. 9, chordamesodermal cells emerge from the node and intercalate in the midline, as the notochordal plate narrows to form the notochord (Sausedo and Schoenwolf, 1994; Sulik et al, 1994). Simultaneously, cells of the overlying neurectoderm converge and intercalate in the midline at all levels of the neuraxis. In the present study, vital labelling of the node with DiI, and labelling the midline neural plate with a GFP expression vector, showed that convergent extension in both chordamesoderm and neural plate is defective in *Lp/Lp* embryos. The result of this developmental defect is that the midline fails to narrow and extend in *Lp/Lp* embryos, unlike in wild type littermates. Although the neural folds form and elevate normally, they are spaced widely apart as result of intervening cells that have not intercalated (Greene et al, 1998). This wide spacing of the neural folds precludes initiation of neural tube closure and leads to severe neural tube defects. It is striking that this mechanism of neural tube closure disturbance appears to be conserved with *Xenopus* embryos in which PCP signalling is disturbed (Wallingford and Harland, 2002).

DiI injection into the node identifies reduced extension in midline mesoderm, whereas more rostral labelling of the notochord does not reveal differences in extension behaviour between *Lp* mutant and wild type embryos. This suggests that while convergent extension is a key factor in the narrowing and elongation of the notochordal plate, immediately in front of the node, elongation of the notochord more rostrally is less dependent on convergent extension. Indeed, morphometric analysis of chick and mouse gastrulation shows that cell rearrangement is a relatively minor contributor to notochord elongation at levels rostral to the notochordal plate (Sausedo and Schoenwolf, 1993; Sausedo and Schoenwolf, 1994).

Longitudinally oriented mitoses appear to account for the majority of the elongation observed in the rostral notochord. We suggest that unimpaired extension of the notochord is the primary factor enabling the limited degree of axial extension that is achieved by *Lp/Lp* embryos.

Defective convergent extension in the *Lp* neural plate could indicate an intrinsic requirement for *Vangl2* function, or a secondary effect of faulty induction by the chordamesoderm. The notochord induces not only expression of floor plate markers such as *Shh* and *netrin-1* in the midline neural plate (Jessell, 2000), but also influences earlier cell morphogenesis. For example, neuroepithelial cells adopt a wedge shape during formation of the median hinge point (MHP) in response to notochordal influence (Smith and Schoenwolf, 1989). Hence, faulty midline cell intercalation in the *Lp/Lp* neural plate could reflect a disturbance of notochordal induction. However, *Vangl2* and other PCP genes are expressed in the early neural plate (Kibar et al, 2001; Murdoch et al, 2001a; Torban et al., 2006), consistent with a direct requirement for PCP signalling during neurectodermal convergent extension. Moreover, our chimera studies suggest that *Lp/Lp* neural plate cells are preferentially affected in convergent extension, compared with wild type cells. If the neural plate defect was secondary to faulty notochordal induction, both wild type and mutant neural plate cells should be equally affected. It seems likely, therefore, that convergent extension requires PCP signalling independently in each germ layer.

The absence of *Lp* mutant cells from the midline of chimeras could reflect a role for *Vangl2* in cell behaviours other than convergent extension. For example, differential cell adhesion may underlie the morphogenetic disturbance in PCP mutant zebrafish (Ciruna et al., 2006). In mouse chimeras, however, differentially adhesive cells tend to show marked spatial segregation (Tam and Rossant, 2003), a phenomenon that we did not observe in *+/+* ⇔ *Lp/Lp* chimeras. It is also possible that the differential abundance of *Lp* mutant and wild type cells in the midline reflects proliferative differences, as in zebrafish PCP mutants where mitotic orientation is disturbed (Gong et al., 2004). However, we previously observed no differences in cell proliferation between *Lp/Lp* and wild type neural plate cells (Gerrelli and Copp, 1997). In the absence of other likely explanations, therefore, the predominance of wild type cells in the midline of *+/+* ⇔ *Lp/Lp* chimeras supports a cell autonomous defect of convergent extension.

PCP signalling via small GTPases regulates intracellular events such as cytoskeletal remodelling that underlie polarised cell behaviour (Klein and Mlodzik, 2005). The apparently cell autonomous effect on convergent extension in *Lp*, with a requirement for RhoA/ROCK signalling, is consistent with this model. However, both cell autonomous and non-cell autonomous features of PCP signalling have been described in other systems. For example, while mediolateral cell alignment during zebrafish convergent extension requires both Vangl2 (Tri/Stbm), and Rho kinase 2 (Rok2), wild type cells also fail to align when transplanted to hosts deficient in Tri/Stbm or Rok2 (Marlow et al, 2002; Jessen et al, 2002). Conversely, overexpression of *Xenopus* Vangl2 (Xstbm) prevents cell intercalation, but can be rescued if overexpressing cells are juxtaposed to wild type cells (Goto and Keller, 2002). In both *Xenopus* and *Drosophila*, non-cell autonomous effects of PCP signalling are generally short-range, often extending a few cell diameters from the edge of single-genotype patches in mosaics (Goto and Keller, 2002; Strutt, 2003). In contrast, mutant and wild type cells were closely intermingled in our mouse chimeras, without distinct patches of either genotype. Hence, the conditions necessary to demonstrate non-cell autonomous effects may have been absent, so that only cell autonomous, single-cell effects were evident.

Neural tube defects are common human malformations, occurring on average in 1 per 1000 pregnancies world wide. While cranial defects are lethal, survivors with spinal

malformations often exhibit considerable disability, starting in childhood and extending into adult life (Botto et al, 1999). Despite their clinical importance, the genetic predisposition to human neural tube defects is poorly understood. The finding that folic acid can prevent a proportion of human neural tube defects (Wald et al., 1991) has prompted studies to seek sequence variants in genes related to folate metabolism, that may be associated with human neural tube defects. The gene encoding 5,10-methylenetetrahydrofolate reductase, a key enzyme in folate metabolism, has yielded a positive correlation with defects in some populations (Van der Put et al., 1997) but, to date, no other genes have been specifically implicated in predisposition to neural tube defects. The same applies to the human orthologues of genes required for neural tube closure in the mouse: although many have been examined, none have so far been implicated in the causation of human malformations (Boyles et al., 2005). Among the PCP genes, sequence variants of *VANGL2* and its family member *VANLG1* were not found to be associated with neural tube defects (Doudney et al, 2005). The present study suggests that other PCP genes should be considered as candidates for a role in the aetiology of human neural tube defects.

Acknowledgments

We thank Juan Pedro Martinez-Barbera for valuable advice and supervision of chimera preparation in the Institute of Child Health ES cell/Gene Targeting Service. Deborah Henderson and Jennifer Murdoch commented on the manuscript, and Jonathan Gilthorpe, Katrin Rittiger, Shuh Narumiya and Elizabeth Robertson provided reagents and cells. This work was supported by the Wellcome Trust and the MRC.

REFERENCES

Ang S-L, Rossant J. *HNF*-3β is essential for node and notochord formation in mouse development. Cell. 1994; 78:561–574. [PubMed: 8069909]

Bastock R, Strutt H, Strutt D. Strabismus is asymmetrically localised and binds to Prickle and Dishevelled during *Drosophila planar* polarity patterning. Development. 2003; 130:3007–3014. [PubMed: 12756182]

Beddington RS, Robertson EJ. An assessment of the developmental potential of embryonic stem cells in the midgestation mouse embryo. Development. 1989; 105:733–737. [PubMed: 2598811]

Beddington RSP. Induction of a second neural axis by the mouse node. Development. 1994; 120:613–620. [PubMed: 8162859]

Botto LD, Moore CA, Khoury MJ, Erickson JD. Neural-tube defects. N. Engl. J. Med. 1999; 341:1509–1519. [PubMed: 10559453]

Boutros M, Paricio N, Strutt DI, Mlodzik M. Dishevelled activates JNK and discriminates between JNK pathways in planar polarity and wingless signaling. Cell. 1998; 94:109–118. [PubMed: 9674432]

Boyles AL, Hammock P, Speer MC. Candidate gene analysis in human neural tube defects. Am. J. Med. Genet. C. Semin. Med. Genet. 2005; 135:9–23. [PubMed: 15816061]

Carroll E, Gerrelli D, Gasca S, Berg E, Beier D, Copp A, Klingensmith J. Cordon-bleu is a conserved gene involved in neural tube formation. Dev. Biol. 2003; 262:16–31. [PubMed: 14512015]

Catala M, Teillet MA, De Robertis EM, Le Douarin NM. A spinal cord fate map in the avian embryo: While regressing, Hensen's node lays down the notochord and floor plate thus joining the spinal cord lateral walls. Development. 1996; 122:2599–2610. [PubMed: 8787735]

Ciruna B, Jenny A, Lee D, Mlodzik M, Schier AF. Planar cell polarity signalling couples cell division and morphogenesis during neurulation. Nature. 2006; 439:220–224. [PubMed: 16407953]

Copp A, Cogram P, Fleming A, Gerrelli D, Henderson D, Hynes A, Kolatsi-Joannou M, Murdoch J, Ybot-Gonzalez P. Neurulation and neural tube closure defects. 1999:135–160.

Copp AJ, Checiu I, Henson JN. Developmental basis of severe neural tube defects in the *loop-tail* (*Lp*) mutant mouse: Use of microsatellite DNA markers to identify embryonic genotype. Dev. Biol. 1994; 165:20–29. [PubMed: 8088438]

Europe PMC Funders Author Manuscripts

Copp AJ, Greene NDE, Murdoch JN. The genetic basis of mammalian neurulation. Nat. Rev. Genet. 2003; 4:784–793. [PubMed: 13679871]

Curtin JA, Quint E, Tsipouri V, Arkell RM, Cattanach B, Copp AJ, Fisher EM, Nolan PM, Steel KP, Brown SDM, Gray IC, Murdoch JN. Mutation of *Celsr1* disrupts planar polarity of inner ear hair cells and causes severe neural tube defects in the mouse. Curr. Biol. 2003; 13:1–20. [PubMed: 12526738]

Darken RS, Scola AM, Rakeman AS, Das G, Mlodzik M, Wilson PA. The planar polarity gene strabismus regulates convergent extension movements in Xenopus. EMBO J. 2002; 21:976–985. [PubMed: 11867525]

Davidson BP, Kinder SJ, Steiner K, Schoenwolf GC, Tam PPL. Impact of node ablation on the morphogenesis of the body axis and the lateral asymmetry of the mouse embryo during early organogenesis. Dev. Biol. 1999; 211:11–26. [PubMed: 10373301]

Doudney K, Ybot-Gonzalez P, Paternotte C, Stevenson RE, Greene ND, Moore GE, Copp AJ, Stanier P. Analysis of the planar cell polarity gene Vangl2 and its co-expressed paralogue Vangl1 in neural tube defect patients. Am. J. Med. Genet. A. 2005; 136A:90–92. [PubMed: 15952208]

Gasca S, Hill DP, Klingensmith J, Rossant J. Characterization of a gene trap insertion into a novel gene, *cordon-bleu,* expressed in axial structures of the gastrulating mouse embryo. Dev. Genet. 1995; 17:141–154. [PubMed: 7586755]

Gerrelli D, Copp AJ. Failure of neural tube closure in the *loop-tail* (*Lp*) mutant mouse: analysis of the embryonic mechanism. Dev. Brain Res. 1997; 102:217–224. [PubMed: 9352104]

Gong Y, Mo C, Fraser SE. Planar cell polarity signalling controls cell division orientation during zebrafish gastrulation. Nature. 2004; 430:689–693. [PubMed: 15254551]

Goto T, Keller R. The planar cell polarity gene Strabismus regulates convergence and extension and neural fold closure in Xenopus. Dev. Biol. 2002; 247:165–181. [PubMed: 12074560]

Greene NDE, Gerrelli D, Van Straaten HWM, Copp AJ. Abnormalities of floor plate, notochord and somite differentiation in the *loop-tail* (*Lp*) mouse: a model of severe neural tube defects. Mech. Dev. 1998; 73:59–72. [PubMed: 9545534]

Greene NDE, Leung KY, Wait R, Begum S, Dunn MJ, Copp AJ. Differential protein expression at the stage of neural tube closure in the mouse embryo. J. Biol. Chem. 2002; 277:41645–41651. [PubMed: 12200422]

Gutjahr MC, Rossy J, Niggli V. Role of Rho, Rac, and Rho-kinase in phosphorylation of myosin light chain, development of polarity, and spontaneous migration of Walker 256 carcinosarcoma cells. Exp. Cell Res. 2005; 308:422–438. [PubMed: 15950966]

Habas R, Kato Y, He X. Wnt/Frizzled activation of Rho regulates vertebrate gastrulation and requires a novel formin homology protein Daam1. Cell. 2001; 107:843–854. [PubMed: 11779461]

Hamblet NS, Lijam N, Ruiz-Lozano P, Wang J, Yang Y, Luo Z, Mei L, Chien KR, Sussman DJ, Wynshaw-Boris A. Dishevelled 2 is essential for cardiac outflow tract development, somite segmentation and neural tube closure. Development. 2002; 129:5827–5838. [PubMed: 12421720]

Jessell TM. Neuronal specification in the spinal cord: inductive signals and transcriptional codes. Nat. Rev. Genet. 2000; 1:20–29. [PubMed: 11262869]

Jessen JR, Topczewski J, Bingham S, Sepich DS, Marlow F, Chandrasekhar A, Solnica-Krezel L. Zebrafish trilobite identifies new roles for Strabismus in gastrulation and neuronal movements. Nat. Cell Biol. 2002; 4:610–615. [PubMed: 12105418]

Keller R. Shaping the vertebrate body plan by polarized embryonic cell movements. Science. 2002; 298:1950–1954. [PubMed: 12471247]

Kibar Z, Vogan KJ, Groulx N, Justice MJ, Underhill DA, Gros P. *Ltap*, a mammalian homolog of *Drosophila Strabismus/Van Gogh*, is altered in the mouse neural tube mutant Loop-tail. Nature Genet. 2001; 28:251–255. [PubMed: 11431695]

Kirillova I, Novikova I, Augé J, Audollent S, Esnault D, Encha-Razavi F, Lazjuk G, Attié-Bitach T, Vekemans M. Expression of the *sonic hedgehog* gene in human embryos with neural tube defects. Teratology. 2000; 61:347–354. [PubMed: 10777830]

Klein TJ, Mlodzik M. Planar cell polarization: an emerging model points in the right direction. Ann. Rev. Cell Dev. Biol. 2005; 21:155–176. [PubMed: 16212491]

Kuan CY, Yang DD, Roy DRS, Davis RJ, Rakic P, Flavell RA. The Jnk1 and Jnk2 protein kinases are required for regional specific apoptosis during early brain development. Neuron. 1999; 22:667–676. [PubMed: 10230788]

Lu X, Borchers AG, Jolicoeur C, Rayburn H, Baker JC, Tessier-Lavigne M. PTK7/CCK-4 is a novel regulator of planar cell polarity in vertebrates. Nature. 2004; 430:93–98. [PubMed: 15229603]

Maekawa M, Ishizaki T, Boku S, Watanabe N, Fujita A, Iwamatsu A, Obinata T, Ohashi K, Mizuno K, Narumiya S. Signaling from Rho to the actin cytoskeleton through protein kinases ROCK and LIM-kinase. Science. 1999; 285:895–898. [PubMed: 10436159]

Marlow F, Topczewski J, Sepich D, Solnica-Krezel L. Zebrafish Rho kinase 2 acts downstream of Wnt11 to mediate cell polarity and effective convergence and extension movements. Curr. Biol. 2002; 12:876–884. [PubMed: 12062050]

Montcouquiol M, Rachel RA, Lanford PJ, Copeland NG, Jenkins NA, Kelley MW. Identification of *Vangl2* and *Scrb1* as planar polarity genes in mammals. Nature. 2003; 423:173–177. [PubMed: 12724779]

Moore CA, Li S, Li Z, Hong SX, Gu HQ, Berry RJ, Mulinare J, Erickson JD. Elevated rates of severe neural tube defects in a high-prevalence area in northern China. Am. J. Med. Genet. 1997; 73:113–118. [PubMed: 9409858]

Murdoch JN, Doudney K, Paternotte C, Copp AJ, Stanier P. Severe neural tube defects in the *loop-tail* mouse result from mutation of *Lpp1*, a novel gene involved in floor plate specification. Hum. Mol. Genet. 2001a; 10:2593–2601. [PubMed: 11709546]

Murdoch JN, Henderson DJ, Doudney K, Gaston-Massuet C, Phillips HM, Paternotte C, Arkell R, Stanier P, Copp AJ. Disruption of *scribble* (*Scrb1*) causes severe neural tube defects in the *circletail* mouse. Hum. Mol. Genet. 2003; 12:87–98. [PubMed: 12499390]

Murdoch JN, Rachel RA, Shah S, Beermann F, Stanier P, Mason CA, Copp AJ. *Circletail*, a new mouse mutant with severe neural tube defects: Chromosomal localisation and interaction with the *loop-tail* mutation. Genomics. 2001b; 78:55–63. [PubMed: 11707073]

Park M, Moon RT. The planar cell-polarity gene stbm regulates cell behaviour and cell fate in vertebrate embryos. Nat. Cell Biol. 2002; 4:20–25. [PubMed: 11780127]

Rachel RA, Murdoch JN, Beermann F, Copp AJ, Mason CA. Retinal axon misrouting at the optic chiasm in mice with neural tube closure defects. Genesis. 2000; 27:32–47. [PubMed: 10862153]

Sausedo RA, Schoenwolf GC. Cell behaviors underlying notochord formation and extension in avian embryos: Quantitative and immunocytochemical studies. Anat. Rec. 1993; 237:58–70. [PubMed: 8214642]

Sausedo RA, Schoenwolf GC. Quantitative analyses of cell behaviors underlying notochord formation and extension in mouse embryos. Anat. Rec. 1994; 239:103–112. [PubMed: 8037374]

Self A, Hall A. Purification of recombinant Rho/Rac/G25K from *Escherichia coli*. Methods Enzymol. 1995; 256:3–10. [PubMed: 7476445]

Smith JL, Schoenwolf GC. Notochordal induction of cell wedging in the chick neural plate and its role in neural tube formation. J. Exp. Zool. 1989; 250:49–62. [PubMed: 2723610]

Stanier P, Henson JN, Eddleston J, Moore GE, Copp AJ. Genetic basis of neural tube defects: the mouse gene *loop-tail* maps to a region of Chromosome 1 syntenic with human 1q21-q23. Genomics. 1995; 26:473–478. [PubMed: 7607670]

Strutt D. Frizzled signalling and cell polarisation in Drosophila and vertebrates. Development. 2003; 130:4501–4513. [PubMed: 12925579]

Strutt DI, Weber U, Mlodzik M. The role of RhoA in tissue polarity and Frizzled signalling. Nature. 1997; 387:292–295. [PubMed: 9153394]

Sulik K, Dehart DB, Inagaki T, Carson JL, Vrablic T, Gesteland K, Schoenwolf GC. Morphogenesis of the murine node and notochordal plate. Dev. Dyn. 1994; 201:260–278. [PubMed: 7881129]

Takeuchi M, Nakabayashi J, Sakaguchi T, Yamamoto TS, Takahashi H, Takeda H, Ueno N. The prickle-related gene in vertebrates is essential for gastrulation cell movements. Curr. Biol. 2003; 13:674–679. [PubMed: 12699625]

Tam PPL, Rossant J. Mouse embryonic chimeras: tools for studying mammalian development. Development. 2003; 130:6155–6163. [PubMed: 14623817]

Torban E, Wang HJ, Groulx N, Gros P. Independent mutations in mouse *Vangl2* that cause neural tube defects in *looptail* mice impair interaction with members of the *Dishevelled* family. J. Biol. Chem. 2004; 279:52703–52713. [PubMed: 15456783]

Torban E, Wang HJ, Patenaude AM, Riccomagno M, Daniels E, Epstein D, Gros P. Tissue, cellular and sub-cellular localization of the Vangl2 protein during embryonic development: Effect of the Lp mutation. Gene Expr. Patterns. 2006 epub.

Van der Put NMJ, Eskes TKAB, Blom HJ. Is the common 677C-->T mutation in the methylenetetrahydrofolate reductase gene a risk factor for neural tube defects? A meta-analysis. Q. J. Med. 1997; 90:111–115.

Wald N, Sneddon J, Densem J, Frost C, Stone R, MRC Vitamin Study Res Group. Prevention of neural tube defects: Results of the Medical Research Council Vitamin Study. Lancet. 1991; 338:131–137. [PubMed: 1677062]

Wallingford JB, Harland RM. *Xenopus* Dishevelled signaling regulates both neural and mesodermal convergent extension: parallel forces elongating the body axis. Development. 2001; 128:2581–2592. [PubMed: 11493574]

Wallingford JB, Harland RM. Neural tube closure requires Dishevelled-dependent convergent extension of the midline. Development. 2002; 129:5815–5825. [PubMed: 12421719]

Wang J, Hamblet NS, Mark S, Dickinson ME, Brinkman BC, Segil N, Fraser SE, Chen P, Wallingford JB, Wynshaw-Boris A. Dishevelled genes mediate a conserved mammalian PCP pathway to regulate convergent extension during neurulation. Development. 2006a; 133:1767–1778. [PubMed: 16571627]

Wang Y, Guo N, Nathans J. The role of Frizzled3 and Frizzled6 in neural tube closure and in the planar polarity of inner-ear sensory hair cells. J. Neurosci. 2006b; 26:2147–2156. [PubMed: 16495441]

Wei L, Roberts W, Wang L, Yamada M, Zhang SX, Zhao ZY, Rivkees SA, Schwartz RJ, Imanaka-Yoshida K. Rho kinases play an obligatory role in vertebrate embryonic organogenesis. Development. 2001; 128:2953–2962. [PubMed: 11532918]

Weinstein DC, Ruiz i Altaba A, Chen WS, Hoodless P, Prezioso VR, Jessell TM, Darnell JE Jr. The winged-helix transcription factor *HNF*-3β is required for notochord development in the mouse embryo. Cell. 1994; 78:575–588. [PubMed: 8069910]

Yamanaka H, Moriguchi T, Masuyama N, Kusakabe M, Hanafusa H, Takada R, Takada S, Nishida E. JNK functions in the non-canonical Wnt pathway to regulate convergent extension movements in vertebrates. EMBO Rep. 2002; 3:69–75. [PubMed: 11751577]

Yaneza M, Gilthorpe JD, Lumsden A, Tucker AS. No evidence for ventrally migrating neural tube cells from the mid- and hindbrain. Dev. Dyn. 2002; 223:163–167. [PubMed: 11803580]

Ybot-Gonzalez P, Cogram P, Gerrelli D, Copp AJ. Sonic hedgehog and the molecular regulation of neural tube closure. Development. 2002; 129:2507–2517. [PubMed: 11973281]

Ybot-Gonzalez P, Copp AJ, Greene NDE. Expression pattern of glypican-4 suggests multiple roles during mouse development. Dev. Dyn. 2005; 233:1013–1017. [PubMed: 15830372]

Zambrowicz BP, Imamoto A, Fiering S, Herzenberg LA, Kerr WG, Soriano P. Disruption of overlapping transcripts in the ROSA βgeo 26 gene trap strain leads to widespread expression of β-galactosidase in mouse embryos and hematopoietic cells. Proc. Natl. Acad. Sci. USA. 1997; 94:3789–3794. [PubMed: 9108056]

Europe PMC Funders Author Manuscripts

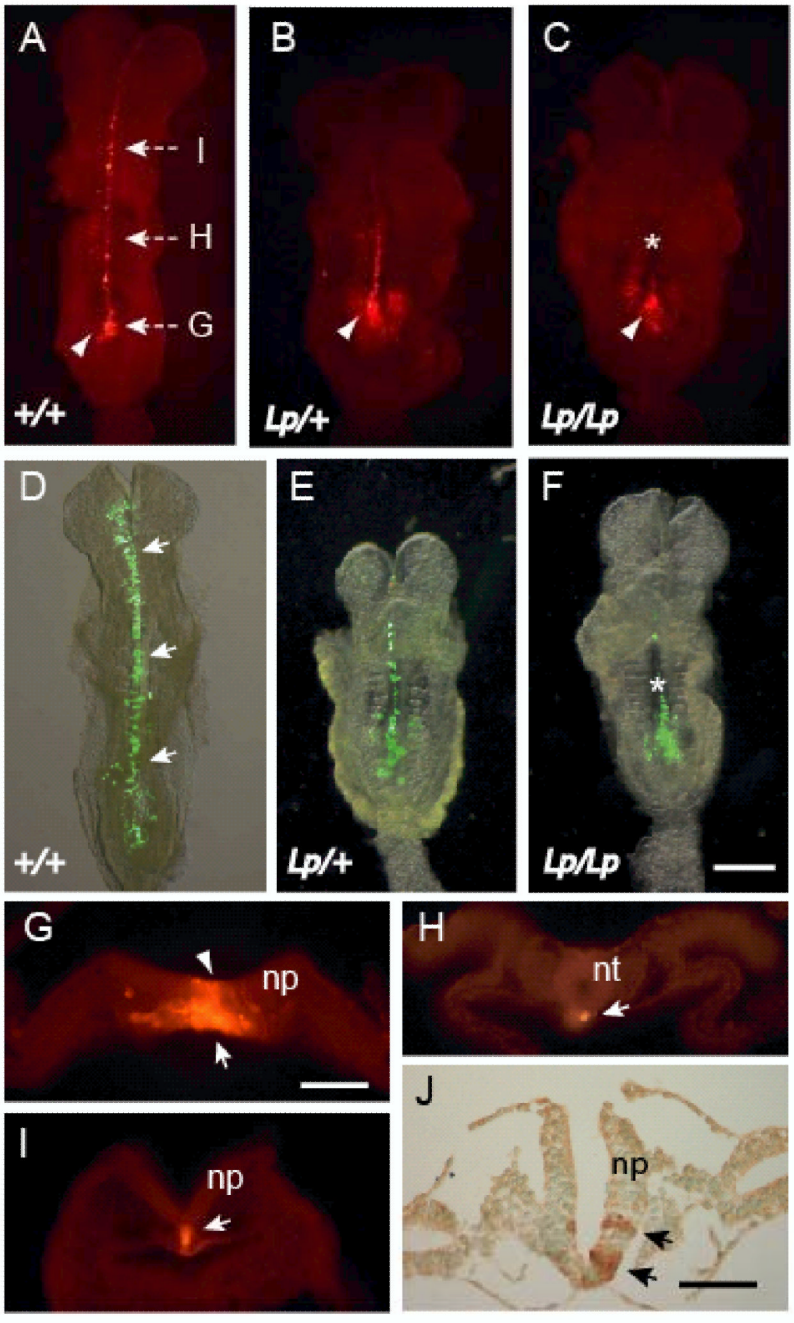

Figure 1.

Defective convergent extension in *Lp* embryos prior to the onset of neural tube closure.

(**A-C**) DiI injection of the node, and (**D-F**) electroporation of a GFP-expressing construct into midline neural plate. Dorsal views (rostral to the top) of DiI or GFP labelled embryos, cultured for 18 h to the 5-7 somite stage. Wild type embryos (A, D) exhibit striking midline extension of DiI or GFP labelled cells (arrows), while *Lp/+* embryos (B, E) exhibit variable midline extension. *Lp/Lp* embryos (C, F) show very limited midline extension, after either DiI or GFP labelling. Arrowheads: DiI injection site in the node; asterisks: open neural tube in *Lp/Lp* embryos. (**G-I**) Transverse sections at axial levels shown in (A) through a wild

type embryo 18 h after DiI injection into the node. Caudally, intense DiI labelling is present in the notochordal plate just rostral to the node (arrow in G) and in a few midline neural plate cells (arrowhead in G). More rostrally, at the level of the closed neural tube (H) and the open hindbrain (I), only the notochord is labelled (arrows in H and I). (**J**) Transverse section through electroporated wild type embryo. Immunostaining with anti-GFP demonstrates labelling in neural plate only (arrows). Abbreviations: np, neural plate; nt, neural tube. Scale bars: 0.5 mm in F (also A-E); 0.1 mm in G (also H, I); 0.05 mm in J.

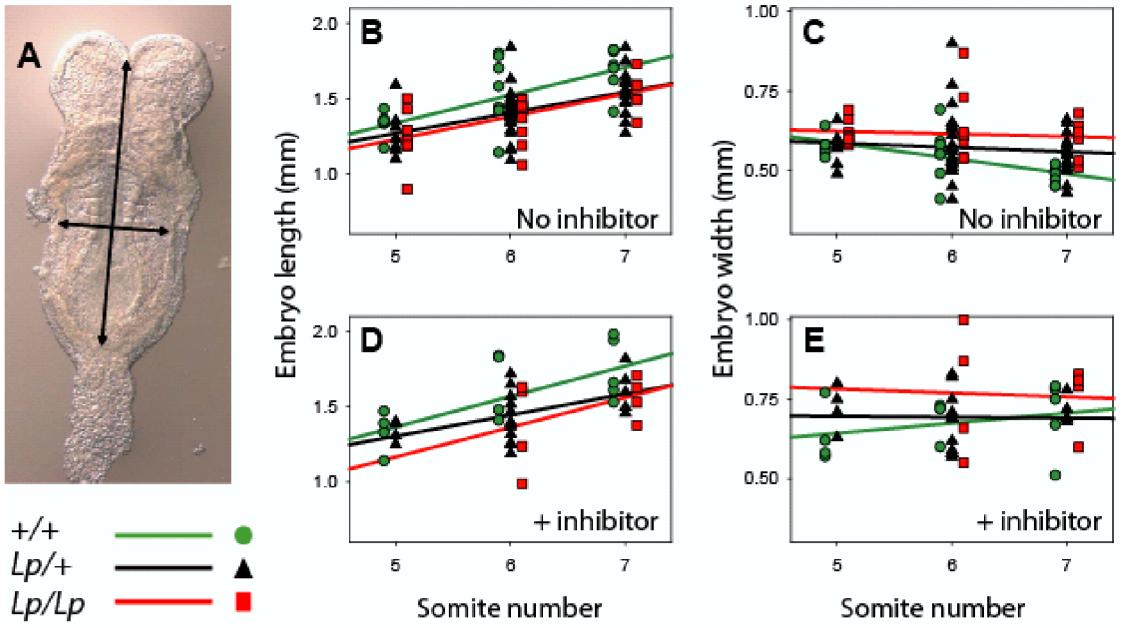

Figure 2.

Diminished length and increased width of *Lp/Lp* embryos. (**A**) Embryonic length and width as measured on photomicrographs of cultured embryos viewed from the dorsal surface, after removal of yolk sac and amnion. (**B-E**) Length and width measurements of embryo cultured in the absence (B,C) or presence (D,E) of the ROCK inhibitor Y27632. Each data point represents a single embryo. Linear regression lines are shown. Embryonic length increases significantly with somite number in both absence (B) and presence (D) of inhibitor (2-way ANOVA; $p < 0.001$). Length also varies significantly with genotype (*+/+* > *Lp/Lp*) in embryos cultured in the absence (B) of inhibitor ($p = 0.008$) whereas, in the presence of inhibitor (D), embryonic length no longer varies significantly with genotype ($p = 0.053$). Embryonic width does not vary significantly with somite number either in the absence (C) or presence (E) of inhibitor ($p > 0.05$). While embryonic width varies significantly between genotypes (*Lp/Lp* > *+/+*) in the absence of inhibitor ($p = 0.006$), there is no significant variation between genotypes in the presence of inhibitor ($p > 0.05$). Embryonic width is significantly greater in the presence of inhibitor (E) than in its absence (C), irrespective of genotype ($p < 0.001$), whereas embryonic length does not differ in the presence (D) or absence (B) of inhibitor ($p > 0.05$). Number of embryos measured in absence/presence of Y27632 is: *+/+*, 35/16; *Lp/+*, 56/25; *Lp/Lp*, 28/11.

Europe PMC Funders Author Manuscripts

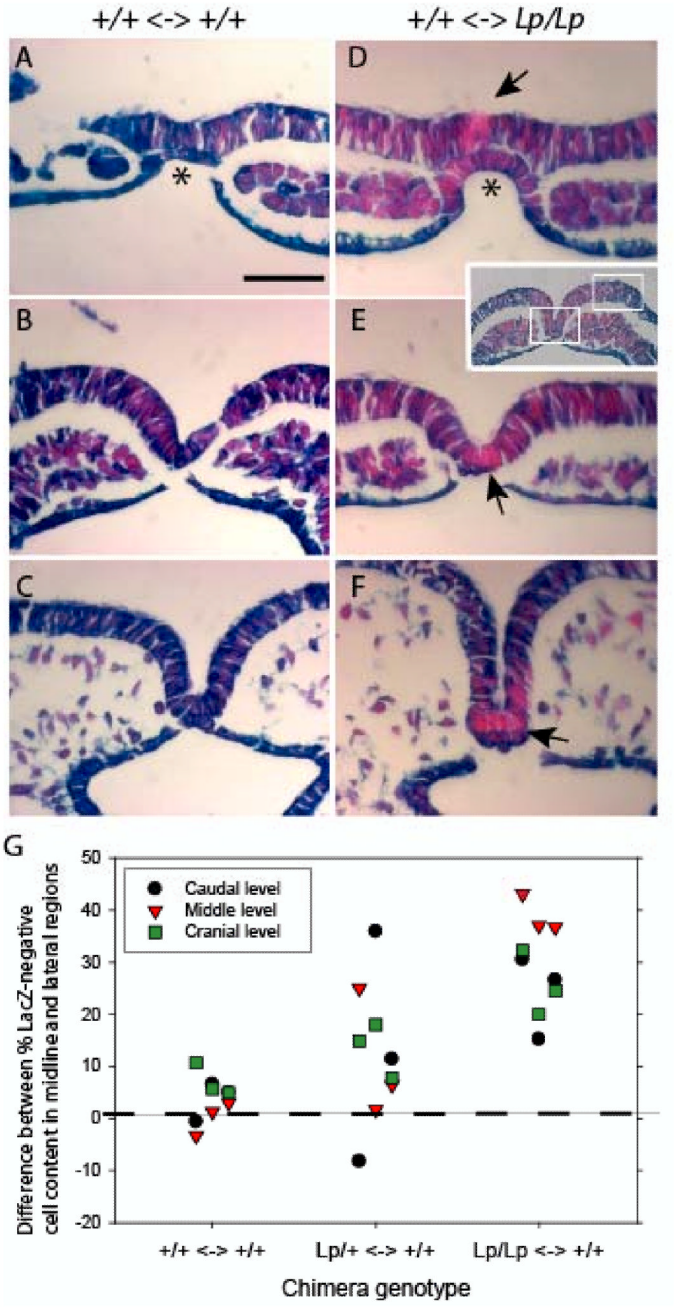

Figure 3.

Cell autonomous defect of convergent extension in the *Lp* mutant as demonstrated in chimeras. (**A-C**) *+/+* ⇔ *+/+* and (**D-F**) *+/+* ⇔ *Lp/Lp* chimeras at E8, produced by injecting wild type ES cells into *Lp* blastocysts that are also homozygous for the ROSA26 LacZ marker. After X-gal staining and eosin counterstaining, all blastocyst-derived cells are blue, while ES-derived cells are pink. Sections at the level of the notochordal plate (A,D), mid-trunk neural folds (B,E) and cranial neural folds (C,F) all show an apparently random admixture of blue and pink cells in *+/+* ⇔ *+/+* chimeras (A-C) whereas *+/+* ⇔ *Lp/Lp* chimeras (D-F) exhibit increased numbers of pink (wild type) cells in the midline of both

neural plate (arrows) and notochordal plate (asterisk in D). More lateral regions show a more even mixture of blue and pink cells. Inset: low magnification view of *+/+* ⇔ *Lp/+* chimera showing boxed areas in which cell counts were made. (**G**) Quantitative analysis of relative cell numbers in midline and lateral neural plate regions of different chimera genotypes. Difference in % LacZ-negative (i.e. wild type) cells between midline and lateral regions gives values close to zero at all axial levels of *+/+* ⇔ *+/+* chimeras whereas *+/+* ⇔ *Lp/Lp* chimeras show values deviating markedly from zero along the entire body axis. *+/+* ⇔ *Lp/+* chimeras show a wide range of values, encompassing the extremes of the other two genotypes. Scale bar: 0.05 mm in A (also B-F).

Europe PMC Funders Author Manuscripts

Europe PMC Funders Author Manuscripts

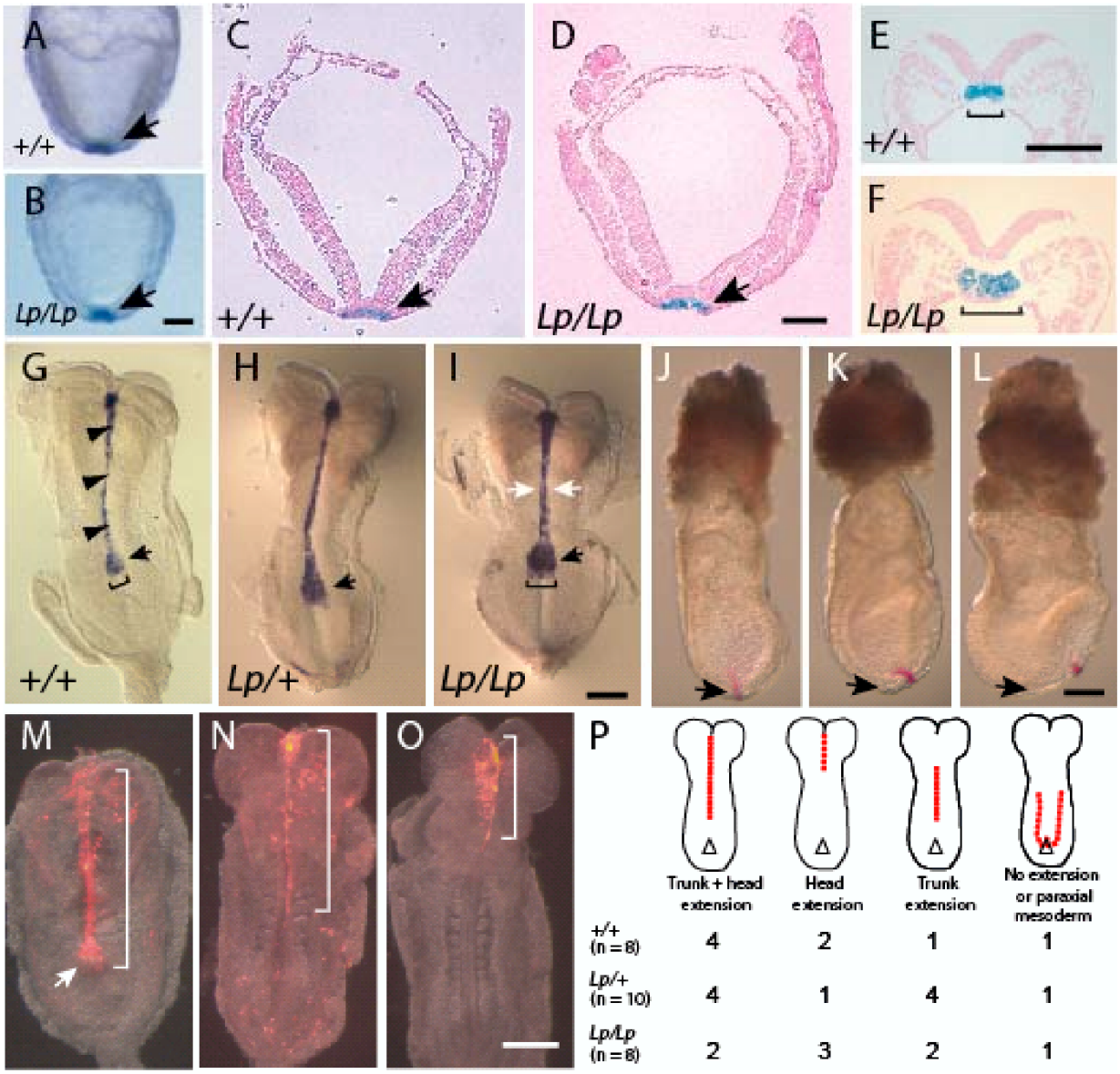

Figure 4.

A node defect but normal notochordal extension in E8.5 *Lp* embryos. (**A-F**) Structure of the node (arrows) in wild type (A,C,E) and *Lp/Lp* (B,D,F) embryos at E7.5 (A-D) and E8.5 (E,F). Embryos are homozygous for the *cordon bleu* (*Cobl*) gene trap which expresses LacZ in the node and its derivatives. At E7.5, whole mounts (A,B) and sections (C,D) show a closely similar structure and LacZ-positive cell number in the node of *+/+* and *Lp/Lp* genotypes. In contrast, at E8.5 the LacZ-positive node appears markedly wider in sections of *Lp/Lp* embryos than in *+/+* litter mates (E,F). (**G-I**) *In situ* hybridisation for *Shh* expression at E8.5 (dorsal view of whole mounts). The node (arrows) is approximately twice as wide in *Lp/Lp* embryos (I) as in *+/+* embryos (G). *Lp/+* embryos have a node of intermediate width (H). The notochordal *Shh* expression domain (arrowheads in G) is also broader in *Lp/Lp* (between white arrows in I) compared with *+/+* and *Lp/+*. (**J-L**) Right lateral view of wild type E7.5 embryos a few minutes after injection of DiI into the node (J), just in front of the

node (K) or further in front of the node (L). Arrows indicate position of node. (**M-O**) After 18 h culture, node-injected embryos exhibit labelling of the entire midline (bracketed region in M), including the triangular node/notochordal plate (white arrow in M). Injection in front of the node yields midline labelling along variable portions of the midline: either trunk + head (N), head only (O), or trunk only (not shown) depending on the precise position of injection and stage of embryo. The triangular node/notochordal plate is not labelled in these embryos. (**P**) Labelling in front of the node (as in K) in embryos from *Lp/+* × *Lp/+* litters yields a range of labelling patterns as in (N,O). The number of *Lp/Lp* embryos with midline extension does not differ significantly from *Lp/+* and *+/+* litter mates. Red dots: DiI labelled cells. Black triangles: node. Scale bars: 0.1 mm in B (also A); 0.1 mm in D (also C); 0.2 mm in E (also F); 0.2 mm in I (also G,H); 0.2 mm in L (also J,K); 0.2 mm in O (also M,N).

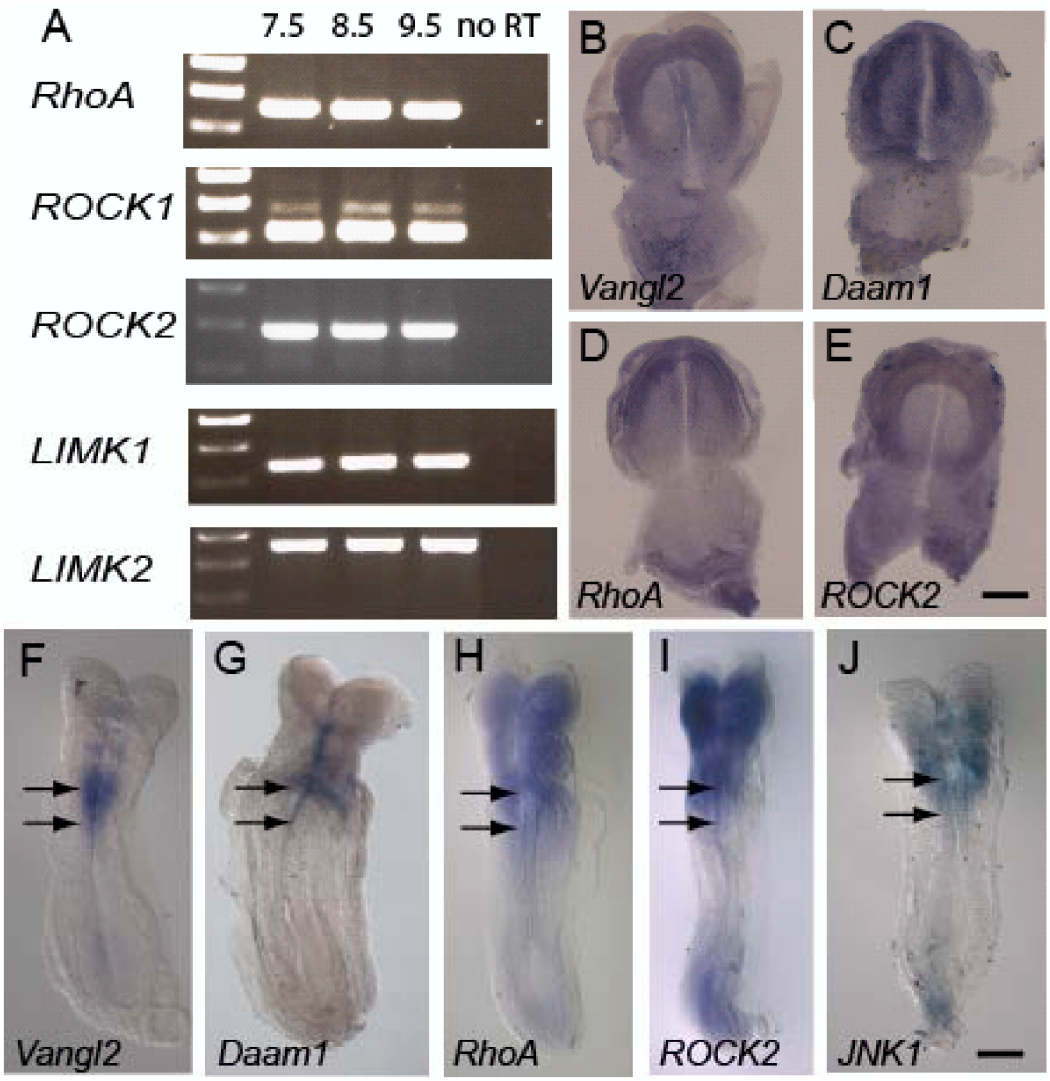

Figure 5.

Expression of RhoA/ROCK and JNK signalling components during mouse neurulation. (**A**) RT-PCR analysis of RhoA, ROCK1, ROCK2, LIMK1 and LIMK2. Lane 1 contains molecular size standards: 800, 600 and 400 bp (top to bottom). Lanes 2-4 show expression in whole embryo homogenates at E7.5, E8.5 and E9.5 respectively. Lane 5 is no RT control. (**B-J**) Whole mount *in situ* hybridisation of wild type embryos at E8 (B-E; pre-somite headfold stage) and at E8.5 (F-J; 5-7 somites). PCP genes *Vangl2* (B) and *Daam1* (C), and the downstream signalling molecules *RhoA* (D), *ROCK2* (E) are expressed throughout the late gastrulation E8 embryo. By E8.5, expression of *Vangl2* (F) and *Daam1* (G) becomes restricted to the hindbrain and upper spinal region, where neural tube closure is initiated (between double arrows in F-J). *RhoA* (H), *ROCK2* (I) and *JNK1* (J) are expressed in overlapping domains with the PCP genes at E8.5. Scale bars: 0.2 mm in E (also B-D); 0.2 mm in J (also F-I).

Europe PMC Funders Author Manuscripts

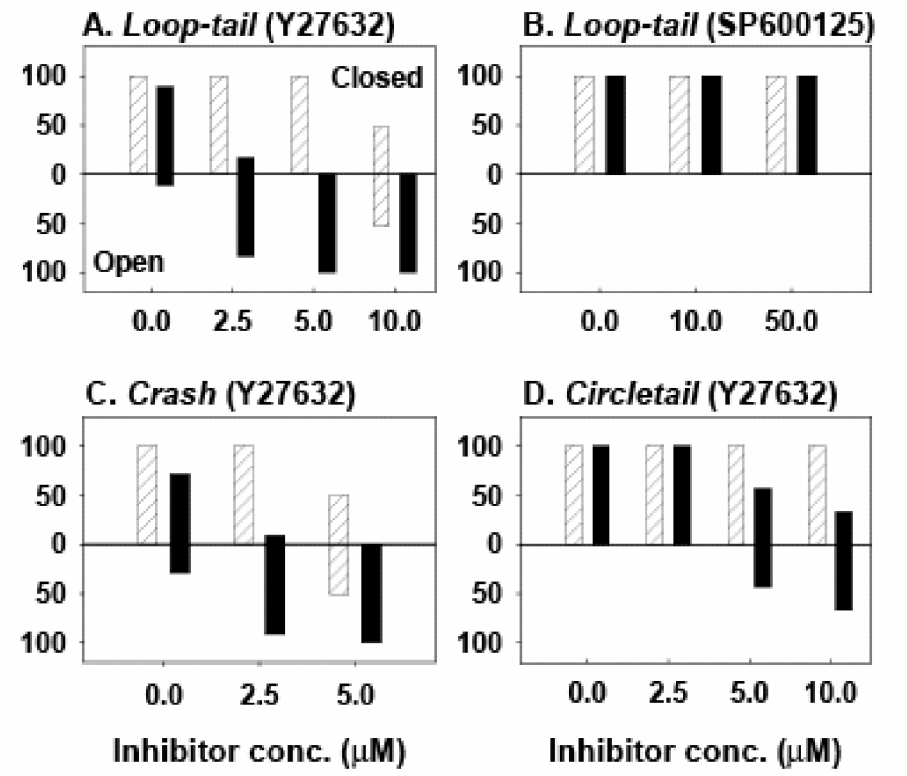

Figure 6.

Interaction between PCP genotype and RhoA/ROCK signalling. Percent embryos with closed neural tube (i.e. successful Closure 1; upward bars) or open neural tube (i.e. failure of Closure 1; downward bars) after 18 h culture from E7.5. Data plotted against concentration of ROCK inhibitor, Y27632, or JNK inhibitor, SP600125. Hatched bars represent *+/+* embryos. Solid bars represent *Lp/+* (A, B), *Crsh/+* (C) and *Crc/+* (D) embryos. While Y27632 affects Closure 1 in wild type embryos only at the highest concentration, and not at all in *circletail* litters, heterozygous embryos of all three strains show failure of Closure 1 at lower Y27632 concentrations. Neurulation is not adversely affected by SP600125 in *+/+* or *Lp/+* embryos. For number of embryos and statistical analysis, see Table 2.

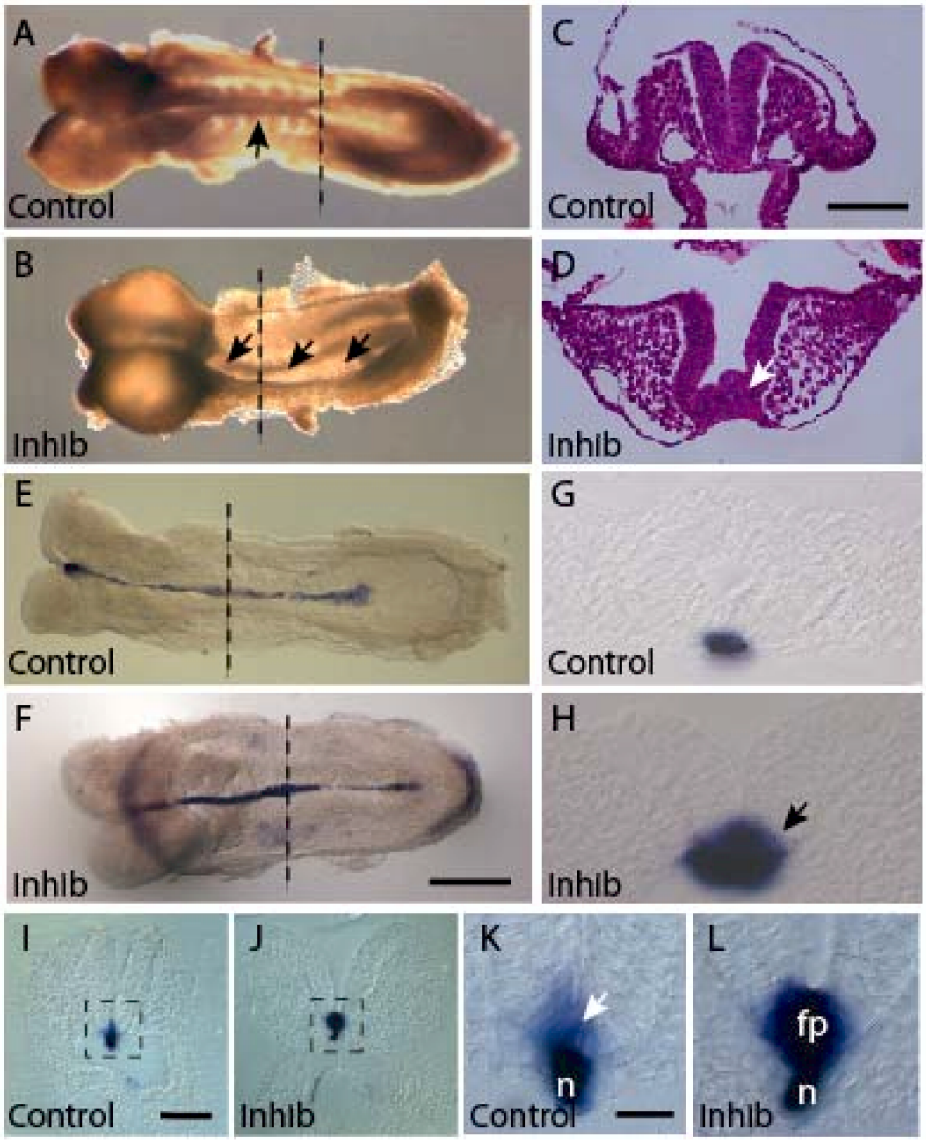

Figure 7.

Expansion of the Shh-positive floor plate in wild type (A-H) and *Lp/+* (I-L) embryos following ROCK inhibition in culture. (**A**) Untreated (control) wild type embryo after successful Closure 1 (arrow). (**B**) Wild type embryo treated with 10 μM Y27632 (Inhib), showing failed Closure 1 (arrows: entirely open neural tube). (**C, D**) H&E staining of transverse sections at the level of the dashed lines in A and B respectively. Note the normal, V-shaped neural fold profile in the untreated embryo (C), in contrast to the broadened floor plate region of the open neural tube after Y27632 treatment (white arrow in D). (**E, F**) Whole mount *in situ* hybridisation for *Shh* in wild type embryos cultured in absence (E) or presence (F) of 10 μM Y27632. Shh expression domain is broader at the site of Closure 1 (dashed lines) in the treated embryo (arrow in F) than in untreated control. (**G, H**) Transverse sections of *Shh* whole mounts, at the level of the dotted lines in E and F respectively. *Shh* expression domain is markedly expanded in the inhibitor-treated embryo (arrow in H). (**I-L**) Sections of *Lp/+* embryos cultured in absence (C) or presence (D) of 2.5 μM Y27632, followed by *in situ* hybridisation for *Shh*. Expression is detected mainly in the

notochord (n) of the untreated control embryo (I; higher magnification in K), with a few positive floor plate cells (white arrow in K). In the inhibitor-treated embryo (J; higher magnification in L), *Shh* is expressed similarly in the notochord but also in a laterally expanded floor plate domain (fp). Scale bars: 0.4 mm in F (also A, B, E), 0.1 mm in C (also D), 0.05 mm in G (also H), 0.1 mm in I (also J), 0.025 mm in K (also L).

Europe PMC Funders Author Manuscripts

Europe PMC Funders Author Manuscripts

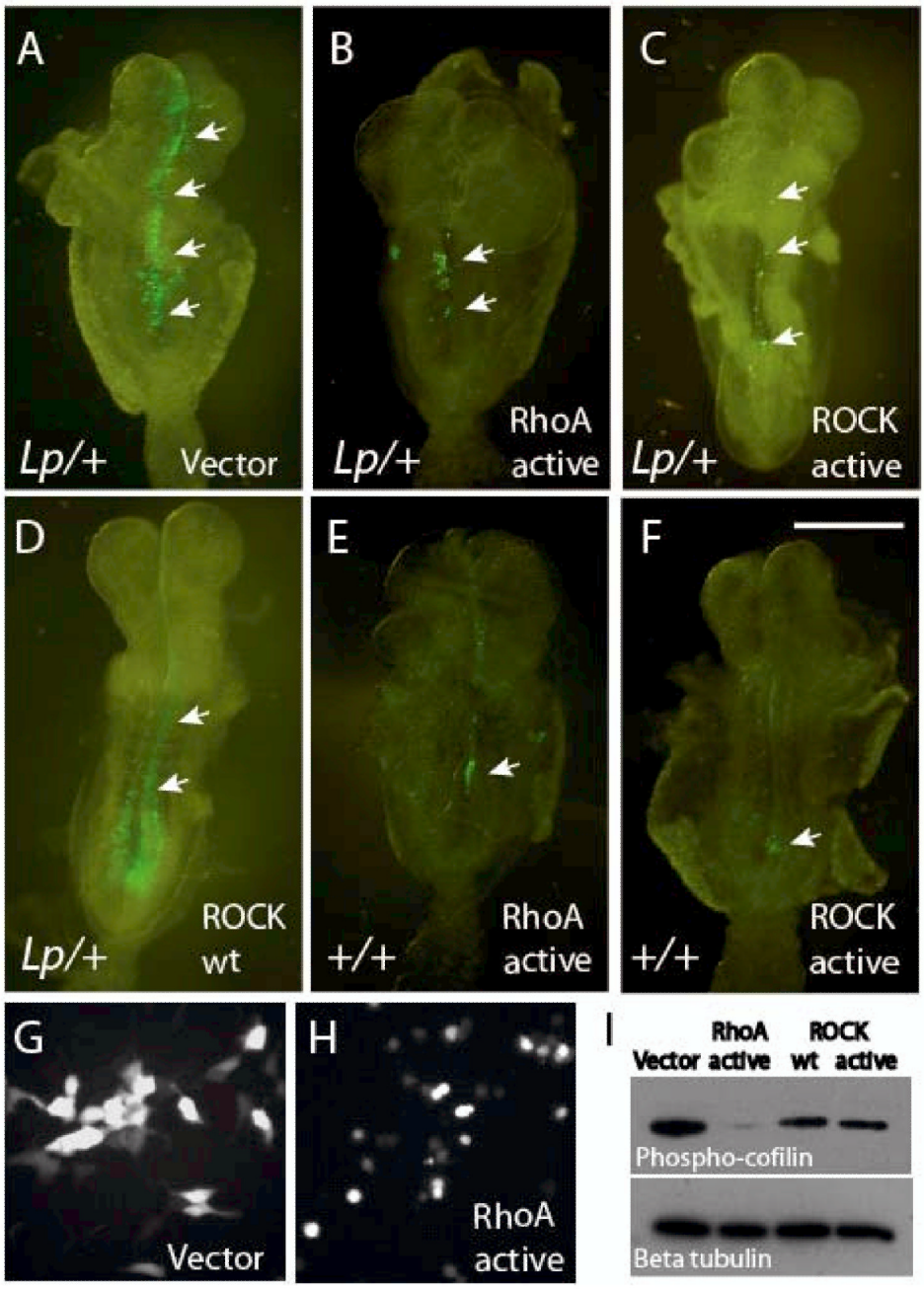

Figure 8.

Electroporation of constitutively active RhoA or ROCK, or wild type ROCK, disrupts convergent extension in *Lp*/+ and +/+ embryos. (**A-F**) *Lp/+* and *+/+* embryos after 18 h culture following electroporation in the node region with vector only (A), RhoA active (B,E), ROCK active (C,F) or ROCK wild type (D). The vector control shows marked midline extension of GFP-positive cells (arrows in A) in contrast to the sparse, clumped appearance of cells electroporated with RhoA active (arrows in B,E) or ROCK active (arrows in C,F). Electroporation with ROCK wild type allows greater midline extension (arrows in D) although less than in the vector control. (**G,H**) 293T cells transfected with

RhoA active (H) show reduced protrusive behaviour compared with vector only controls (G). (**I**) Immunoblot for phosphorylated cofilin in 293T cells transfected with vector only (lane 1), RhoA active (lane 2), ROCK wild type (lane 3) or ROCK active (lane 4). Beta tubulin (lower panel) serves as a loading control. Note the severely reduced phosphocofilin abundance in cells expressing constitutively active RhoA and mild down regulation of phosphocofilin in cells expressing wild type and constitutively active ROCK. Scale bar: 0.4 mm in F (also A-E).

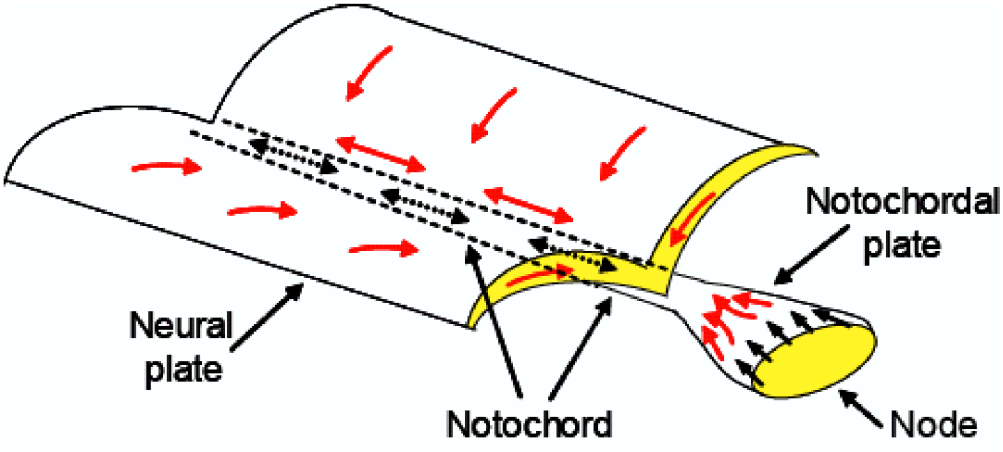

Figure 9.

Summary of the convergent extension defect in *Lp*. Mesodermal cells emerge from the node into the notochordal plate where midline intercalation leads to narrowing to form the notochord. In the overlying neural plate, cells converge on the midline where they extend in the rostro-caudal axis. Red arrows: events that are disrupted in *Lp/Lp* embryos: principally midline intercalation in cells emerging from the node and convergent extension in the neural plate. Black arrows: events that appear to occur normally in *Lp/Lp* embryos.

Europe PMC Funders Author Manuscripts

Table 1

Frequency of rostrally-directed extension of labelled cells following injection of DiI or electroporation of a GFP expression vector into *+/+*, *Lp/+* and *Lp/Lp* embryos at E7.5, followed by 18 h development in whole embryo culture (see also Fig. 1)

	Number of embryos (% total)		
	No midline extension *	**Midline extension** *	**Total**
1. DiI injected embryos			
+/+	2 (6%)	33 (94%)	35
Lp/+	12 (21%)	46 (79%)	58
Lp/Lp	18 (53%)	16 (47%)	34
2. GFP electroporated embryos			
+/+	0 (0%)	8 (100%)	8
Lp/+	3 (25%)	9 (75%)	12
Lp/Lp	13 (100%)	0 (0%)	13

* Proportion of embryos undergoing midline extension differs significantly between genotypes ($p < 0.001$) for both DiI and GFP labelling methods.

Europe PMC Funders Author Manuscripts

Table 2

Frequency of open neural tubes (failure of Closure 1) among wild type and heterozygous embryos of the *Lp*, *Crsh* and *Crc* mutant strains treated with Y27632 and SP600125

			No. open neural tubes/Total no. embryos		
Gene	**Inhibitor**	**Conc (μ M)**	**Wild type**	**Heterozygote**	**Z test [1]**
Lp	Y27632	0	0/24	1/9	
		2.5	0/5	5/6	*
		5	0/8	11/11	*
		10	22/42	7/7	
	SP600125	0	0/15	0/6	
		10	0/9	0/3	
		50	0/5	0/5	
Crsh	Y27632	0	0/5	2/7	
		2.5	0/4	10/11	*
		5	2/4	2/2	
Crc	Y27632	0	0/10	0/17	
		2.5	0/5	0/7	
		5	0/11	3/7	
		10	0/6	6/9	*

[1] Asterisk indicates a significant difference between proportion of open neural tubes in wild type and heterozygous embryos by Z-test, $p < 0.05$.

Europe PMC Funders Author Manuscripts

Table 3

Frequency of open neural tubes (failure of Closure 1) among *+/+*, *Lp/+* and *Lp/Lp* embryos electroporated with vectors expressing constitutively active RhoA or ROCK, or wild type ROCK

	No. embryos with open neural tube/Total no. embryos		
Construct	**+/+**	***Lp*/+**	***Lp/Lp***
Empty vector	0/3	1/4	1/1
RhoA active	4/10	4/7	3/3
ROCK active	2/4	5/6	3/3
ROCK wild type	1/4	2/9	1/1